ACS OMEGA

Article

Cite This: ACS Omega 2018, 3, 7523−7531

Facile Preparation of Tannic Acid−Poly(vinyl alcohol)/Sodium Alginate Hydrogel Beads for Methylene Blue Removal from Simulated Solution

Tao Hu,[†] Qinze Liu,*[,†,‡] Tingting Gao,[§] Kaijie Dong,[†] Gang Wei,[†] and Jinshui Yao*[,†]

[†]School of Materials Science and Engineering and [§]Key Laboratory of Fine Chemicals in Universities of Shandong, School of Chemistry and Pharmaceutical Engineering, Qilu University of Technology (Shandong Academy of Sciences), Jinan 250353, PR China

[‡]State Key Laboratory of Solid Lubrication, Lanzhou Institute of Chemical Physics, Chinese Academy of Sciences, Lanzhou 730000, PR China

Supporting Information

ABSTRACT: A novel hydrogel bead [tannic acid (TA)−poly(vinyl alcohol) (PVA)/sodium alginate (SA)] with high strength prepared by biocompatible PVA, TA, and biocompatible SA via an instantaneous gelation method was applied to remove methylene blue (MB) from aqueous solution. The obtained TA−PVA/SA hydrogel beads were fully characterized by thermogravimetric analysis, Fourier-transform infrared spectroscopy, X-ray photoelectron spectroscopy, scanning electron microscopy, and so on. The adsorption performances of TA−PVA/SA hydrogel beads for MB were investigated by changing the factors of TA content, initial concentration, pH, adsorbent dosage, contact time, and temperature systematically. The maximum capacity of TA−PVA/SA hydrogel beads for MB removal was obtained to be 147.06 mg/g at 30 °C, whose capability was better than that without TA. After fitting the adsorbed data, it was basically consistent with the Langmuir isotherm and pseudo-second-order kinetic model. Thermodynamic studies indicated that MB removal was spontaneous and exothermic in nature. It is concluded that the low-cost TA−PVA/SA hydrogel beads as an easily recoverable adsorbent have a great potential on the removal of hazardous dyes from wastewater.

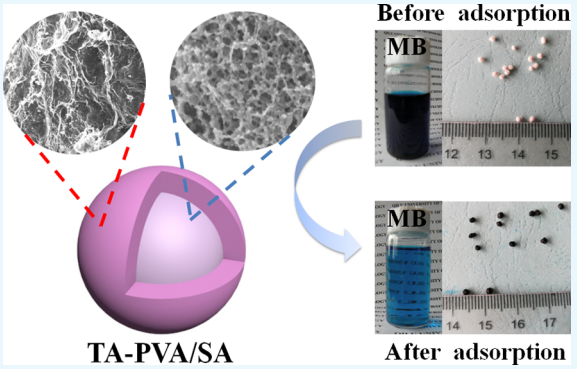

INTRODUCTION

When dyes are used to beautify the world, the wastewater containing these hazardous materials produced from many manufactories using dyes to whitewash their products, for example, textile, dyestuffs, paper, and plastic, are wantonly spread into the biosphere.[1] Once a certain amount of dyes or their degradation substances enter into human body, the toxins can endanger people's health and even cause a variety of diseases, for instance, cancer, deformity, mutation, and so on[2] Methylene blue (MB) as a common cationic dye is widely used in the field of textile, food, paper, printing, and pharmaceutical industries, which is very harmful for the organism because it can easily be associated with oppositely charged cell membrane surfaces.[3] Furthermore, the color value of MB is very high, and it is clearly colored inside; although the concentration is low (<1 mg/L), it is still considered as a toxic colorant.[4] Therefore, the removal of MB from wastewater is an important environmental problem. Therefore, the dyes containing wastewater must be fully treated before it is discharged into the environment.

So far, several conventional approaches have been developed to remove MB from the simulated solution, including biological methods, coagulation and flocculation,[5] chemical oxidation,[6] membrane filtration,[7] photocatalysis,[8] and adsorption.[9] Among this, adsorption is a flexible, simple, and effective method.[10] It is worth noting that the key to adsorption is to find an adsorbent with high removal rate and low cost. It plays a decisive role in the removal of toxic substances.[11]

In recent years, the three-dimensional network polymeric hydrogel used as adsorbents has attracted wide attention.[12] During the removal process, the dye molecules can quickly permeate into the hydrogel network in solution and then combine with the hydrophilic functional groups in its body, for example, −OH. Therefore, the hydrogel adsorbents have good adsorption properties and a great potential in practical applications of water purification.[13,14] Recently, PVA poly(vinyl alcohol) hydrogels have been used more and more in the field of sewage treatment because of their good mechanical strength, chemical stability, hydrophilicity, high biocompatibility, biodegradability, and so on.[15] At the same time, its

Received: March 26, 2018
Accepted: June 18, 2018
Published: July 9, 2018

DOI: 10.1021/acsomega.8b00577
ACS Omega 2018, 3, 7523−7531

structural integrity can be maintained during the deformation.[16] As the report goes, a type of PVA hydrogel beads are considered to be the adsorbent for the feasibility of adsorbing MB dyes.[15] The hydroxyl group in the adsorbents plays a positive role because it has great affinities to cationic MB after taking a negative charge. Agarwal et al. studied PVA to remove bromothymol blue and MB from wastewater.[17] Tannic acid (TA) is one of the natural organic matter because a complex compound of polyphenol contains a number of *o*-dihydroxy and trihydroxy aromatic ring structures. This structure has given it a series of unique chemical properties.[18] Its benzene ring can produce $\pi-\pi$ conjugate with the benzene ring of the dye molecule.[19] Nevertheless, TA is a water-soluble compound and has the disadvantage of being leached by water when it used directly as an adsorbent.[20] Bertagnolli et al. immobilized TA via polyethylenimine to achieve effective adsorption of boron.[21] It is worth mentioning that TA is involved in the mixed solution of PVA and sodium alginate (SA) to form TA−PVA/SA hydrogel beads, which can be utilized to purify the MB dye from sewage. TA can increase the adsorption capacity and thermal stability. The reaction between SA and $CaCl_2$ can form a shell of hydrogel beads, and the cross-linking of boric acid with hydroxyl groups on PVA can further improve the stability of hydrogel beads.

In this work, novel hydrogel beads were prepared easily via an instantaneous gelation method and applied to the removal of MB from aqueous solution. The assembled hydrogel beads were characterized by thermogravimetric analysis (TGA), Fourier transform infrared spectrometer (FT-IR), scanning electron microscopy (SEM), and X-ray photoelectron spectroscopy (XPS). Many factors affecting the MB adsorption from the simulated solution by TA−PVA/SA hydrogel beads were studied in detail, including different TA contents, pH values, contact time, initial concentration, different adsorbent dosage, environmental temperature, and competitive ions. Besides, adsorption kinetics, adsorption isotherms, intraparticle diffusion, and thermodynamic analyses are further analyzed. Finally, the optimal adsorption conditions will be obtained.

RESULTS AND DISCUSSION

Characterization of Hydrogel Bead. The surface and cross-sectional SEM images of TA−PVA/SA hydrogel beads are presented in Figure 1. The diameter of the hydrogel beads mainly ranges from 1.0 to 1.5 mm. As shown in Figure 1b, the surface of TA−PVA/SA beads is an irregular gully shape. As is presented in Figure 1d, the inner part of TA−PVA/SA can be a three-dimensional network structure with lots of open pores; this may be because of the hydrogen bonding between the phenolic hydroxyl group in the TA molecule and the alcoholic hydroxyl group in the PVA chain.[22] These structures will provide a convenient diffusion channel benefit to remove MB dye by TA−PVA/SA beads.

Figure 2a presents the FT-IR spectra of pure PVA, SA, TA, and the TA−PVA/SA hydrogel beads. In the spectrum of TA−PVA/SA hydrogel, the peaks at 1200 and 1320 cm^{-1} are mainly supported by TA, the bands at 2900−2950 cm^{-1} are mainly because of PVA,[23] and the bands ranging from 1560 to 1740 cm^{-1} are attributed to SA. As shown in Figure S1b, the color reaction between $FeCl_3$ and TA−PVA/SA hydrogel beads further confirmed the successful immobilization of TA on the hydrogel beads. The results indicate that the hydrogels are prepared by TA, SA, and PVA successfully.

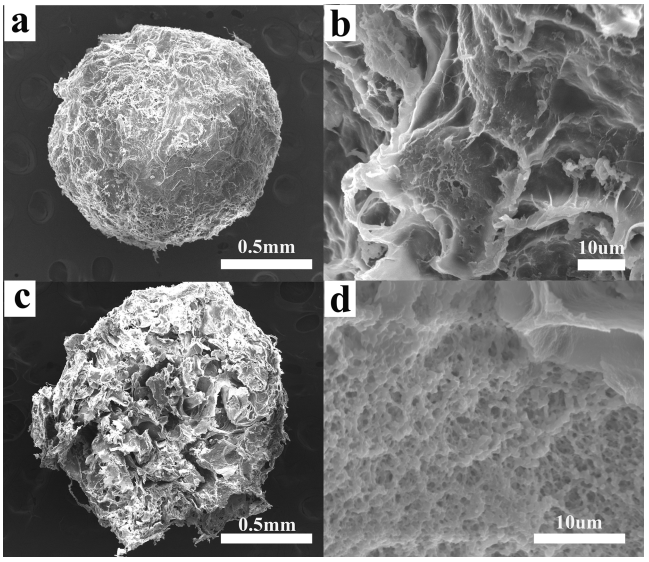

Figure 1. SEM images of the TA−PVA/SA hydrogel beads adsorbent: (a) surface, (b) surface magnification, (c) cross section, and (d) cross-sectional magnification.

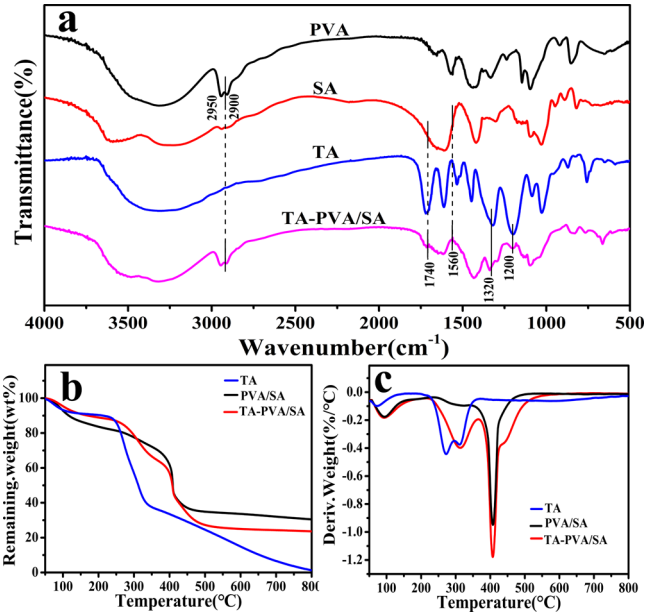

Figure 2. (a) FT-IR spectra, (b) TGA, and (c) derivative thermogravimetric curves of the TA, PVA/SA, and TA−PVA/SA hydrogel beads.

The TGA of the TA, PVA/SA, and TA−PVA/SA hydrogel beads is shown in Figure 2b,c. It is presented that the first weight loss below 120 °C is mainly because of the water evaporation that is adsorbed on materials. With the increase of heating temperature, the TGA curves of TA and two kinds of hydrogel beads (Figure 2a,b) show different stages. For TA, the second mass loss lying in between 230 and 360 °C is attributed to the decomposition of groups (e.g., oxygen-containing groups) and the oxidation of carbon, and the third mass loss corresponds to thermal decomposition.[24] For PVA/SA, the second mass loss lies in between 150 and 430 °C and the third loss falls into the range from 430 to 460 °C. For TA−PVA/SA gel, the second mass loss ranges from 240 to 420 °C, which is mainly because of TA, and the third mass loss ranges

DOI: 10.1021/acsomega.8b00577
ACS Omega 2018, 3, 7523−7531

from 420 to 500 °C, which is mainly because of PVA/SA.[17] It can be seen that TA is successfully introduced into TA−PVA/SA beads by comparing the thermogravimetric curve of TA−PVA/SA hydrogel beads with that of PVA/SA and TA.

The TA−PVA/SA beads before and after adsorbing MB were characterized by XPS to evaluate the element of the dye, and the results are shown in Figure 3. Compared to the peaks of O 1s, C 1s, and Ca 2p in TA−PVA/SA beads, the TA−PVA/SA bead-loaded MB can clearly observe S 2p and N 1s, which are special elements of the MB dye. The results confirm that the dye has been absorbed on the TA−PVA/SA hydrogel beads adsorbent.

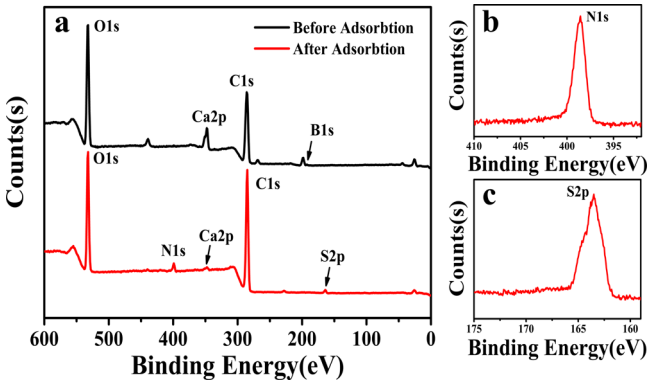

Figure 3. XPS survey spectra of TA−PVA/SA hydrogel beads before and after adsorption of dyes (a), and the amplified spectra of N 1s (b) and S 2p (c) after adsorption.

Effect of Different TA Content on MB Absorption. TA−PVA/SA hydrogel beads containing different amounts which were prepared in laboratory under the same conditions were compared to the adsorption properties. As shown in Figure 4a, the hydrogel beads without TA and the adsorption amount of MB on microspheres is the lowest. With the increase of TA ratio, the adsorption capacity of TA−PVA/SA hydrogel beads increases gradually. When the ratio reaches 1:0.11, the amount of adsorption reaches 147.06 mg/g. This is because TA contains a large number of phenolic hydroxyl groups (−OH), which can hydrolyze to anions ($-O^-$) under basic condition, and the interaction with MB is stronger. Thus, it can be inferred that the proportion of TA is increased from 0 to 0.11, and the more −OH contained in the hydrogel beads adsorbent, the more MB dye is adsorbed. Further increase of TA content, the mixed solution (containing TA, PVA, and SA) is too viscous to drop into solution (3% $CaCl_2$-saturated boric acid) to prepare the TA−PVA/SA hydrogel beads. Therefore, the TA−PVA/SA beads adsorbent with the ratio of TA−PVA to 0.11:1 is used to adsorb MB dye.

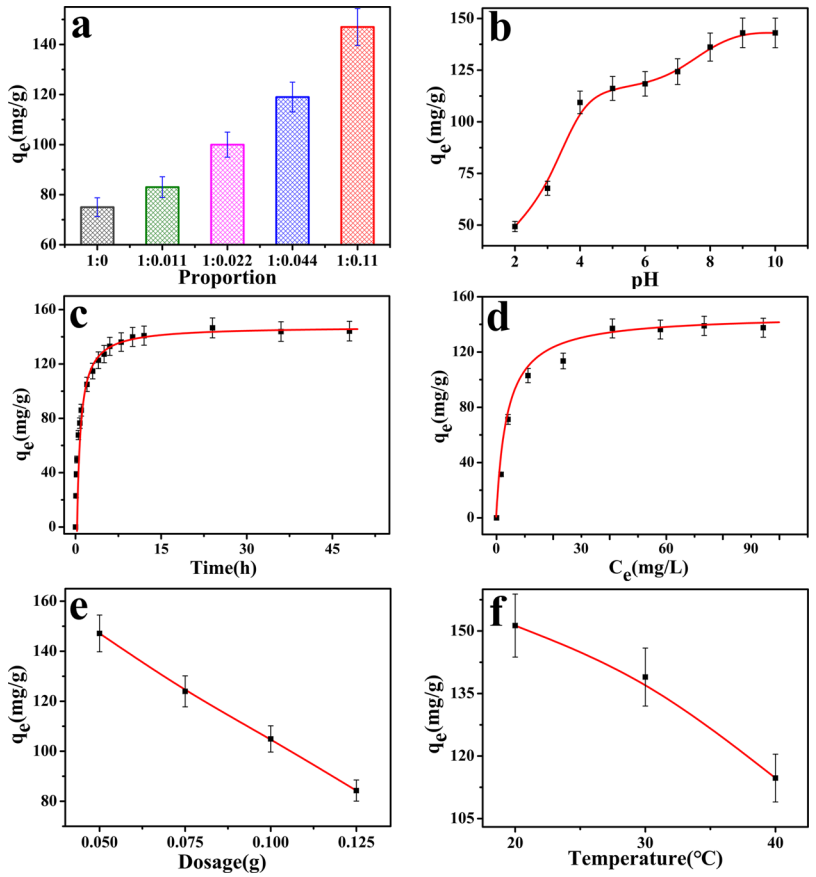

Figure 4. Effects of different factors on the adsorption amount of MB onto the TA−PVA/SA hydrogel beads: (a) TA content in TA−PVA/SA hydrogel (cond. proportion = 1:0, 1:0.011, 1:0.022, 1:0.044, 1:0.11, C_0[MB] = 120 mg/L, V = 100 mL, T = 30 °C, t = 12 h, dos. = 50 mg), (b) pH (cond. pH = 2−10, C_0[MB] = 120 mg/L, V = 100 mL, T = 30 °C, t = 12 h, dos. = 50 mg), (c) contact time (cond. t = 0−48 h, C_0[MB] = 120 mg/L, V = 100 mL, T = 30 °C, t = 12 h, pH = 9, dos. = 50 mg), (d) initial concentration (cond. C_0 = 20−160 mg/L, V = 100 mL, T = 30 °C, t = 12 h, pH = 9, dos. = 50 mg), (e) adsorbent dosage (cond. dos. = 50−125 mg, C_0[MB] = 120 mg/L, V = 100 mL, T = 30 °C, t = 12 h, pH = 9), and (f) temperature environment (cond. T = 20−40 °C, C_0[MB] = 120 mg/L, V = 100 mL, t = 12 h, pH = 9, dos. = 50 mg).

DOI: 10.1021/acsomega.8b00577
ACS Omega 2018, 3, 7523−7531

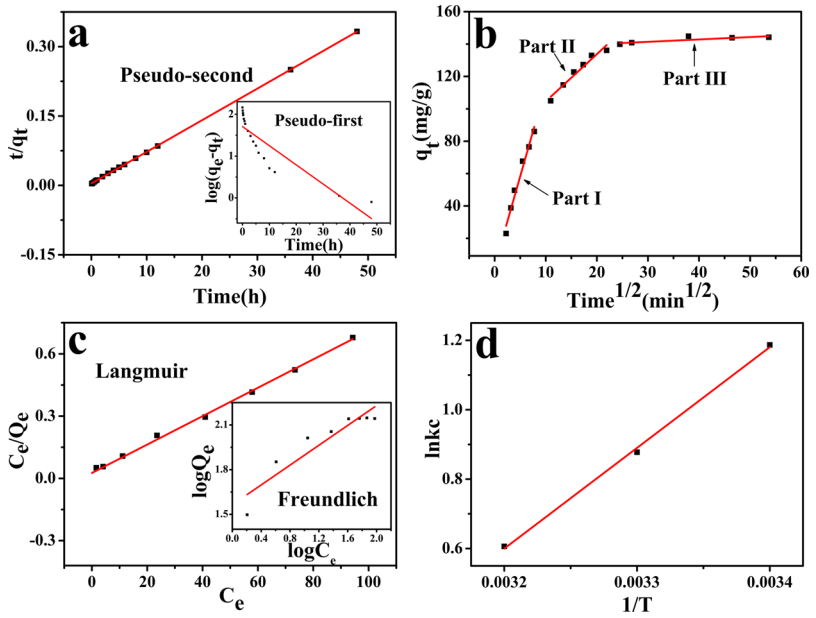

Figure 5. (a) Kinetic models, (b) intraparticle diffusion model, (c) isotherm models, and (d) thermodynamics analysis of the MB removal from pH-regulated solution.

Effect of pH on MB Absorption. The pH of the dye solution may affect the dissociation of functional groups such as alcoholic hydroxyl groups and phenolic hydroxyl groups which worked as the active sites of the adsorbent.[25] The adsorption experiments of MB on TA−PVA/SA hydrogel beads are conducted in different pH ranging from 2.0 to 10.0, and the results are presented in Figure 4b. It could be seen that the MB adsorption was highly pH-dependent, and the adsorption of MB on TA−PVA/SA hydrogel beads is favored at higher pH value. The MB adsorption amount on TA−PVA/SA hydrogel beads obviously increased from 49.3 to 143.0 mg/g as the solution pH increase from 2.0 to 10.0. It has been reported that MB is a weak base and only reacts in strong acid solutions to produce small amounts of protonated cations. Therefore, it is certain that within the weakly basic pH range in question, MB is a positively charged cation which is not protonated.[26] When the pH of the solution is low, TA was mainly in the form of molecules, and the force between MB and TA is weak. When the pH of the solution increases gradually, TA can be partially dissociated into negative charge anions ($-O^-$), interacting with the positive-charged MB stronger, thus, resulting in the increase of the adsorption amount.

Effect of Contact Time on MB Absorption. Contact time is an important factor that indicates whether the adsorbent removes the target contaminant to reach the equilibrium.[27] Figure 4c shows the relationship between contact time and the TA−PVA/SA hydrogel beads' capacities to adsorb MB. First of all, the q_t increases fast within a short time, for example, the removal amount reached 104.96 mg/g with 2 h. The adsorption amounts reached about 140.86 mg/g when the contact time is 12 h. Finally, the q_t tends to be stable at 12−48 h, and the adsorption capacities of the MB reach 144.19 mg/g. The adsorption amounts a rapid increase initially owing to the high probability of the MB occupying site and the excess active sites on the hydrogel beads. With the prolongation of time, the sites on the adsorbents are occupied; the probability of interaction between MB and the adsorption sites are lower; and the adsorption gradually slows down and eventually tended to balance.

Effect of Initial Concentration on MB Absorption. The removal amount is significantly affected by the initial concentrations of dye solution.[28] It is noteworthy that, as the concentration increases, the adsorption amount increases rapidly, until an inflection point occurs and the amount of adsorption tends to be stable. The removal amount is 137.1 mg/g at 100 mg/L MB dye initial concentration, which increases to 139 mg/g at 140 mg/L initial concentration (Figure 4d). Its adsorption amount is quite similar. The initial concentration is an important information for exploring the adsorption capacity of adsorbents.[29] At lower initial concentrations, the adsorbents are relatively over-dosed and the sites are occupied. With the increase of initial concentration, the adsorption capacity increases gradually, and the sites are gradually occupied. At higher concentrations, MB is relatively excessive, and the sites of the adsorbents are almost all occupied. Even if the initial concentration of MB solution is increased further, the TA−PVA/SA beads will not supply more active sites for the MB molecules.[30]

Effect of Adsorbent Dosage on MB Absorption. The effect of different TA−PVA/SA dosages on the adsorption process is studied. Figure 4e shows the relationship between removal amount of the MB and the dosage of TA−PVA/SA beads, and the removal amount decreased from 147 to 84 mg/g as the dosage of TA−PVA/SA beads increased. Because the initial MB concentration is fixed, when the TA−PVA/SA hydrogel beads adsorbent amount increased, the total adsorption amount of MB beads on the hydrogel beads increases, but the adsorption amount per unit mass of TA−PVA/SA beads is decreasing, and the utilization of adsorbent would be greatly reduced. Therefore, the dosage of 50 mg TA−PVA/SA hydrogel bead adsorbents are selected for other experiments.

Effect of Temperature on MB Absorption. The effect of temperature on the removal amount is an important factor to study dye adsorption in industrial wastewater at different

DOI: 10.1021/acsomega.8b00577
ACS Omega 2018, 3, 7523−7531

Table 1. Parameters of Kinetic Models for MB Removal by TA−PVA/SA Hydrogel Beads

adsorbate	pseudo-first-order model			pseudo-second-order model		
	K_1 $(h^{-1})/(mg/L)^{1/n}$	q_e (mg/g)	R^2	K_2 (g/mg h)	q_e (mg/g)	R^2
MB	0.103	50.76	0.7634	0.011	146.19	0.9999

temperatures. Figure 4f shows the relationship between temperature and removal amount of the MB. Obviously, the MB dye removal capacity decreases as the temperature rises from 20 to 40 °C, which reveals that MB dye adsorption is exothermic in nature. The decrease in adsorption amount might be because of the increased solubility of MB with the temperature risen which causes the dissociation of the adsorbed dyes. Another possible reason is that the enhanced interaction of TA and PVA may reduce some of the active adsorption sites at higher temperatures and thus reduce the adsorption amount.[31]

Effect of Competitive Ions on MB Removal. Dye industrial wastewater contains a variety of impurities and MB coexists, such as metal ions, salts, acids, and alkalis. Therefore, removing MB from wastewater containing competitive ions is of great significance to environmental safety. It has been reported that the presence of competing ions may affect the adsorbent's adsorption capacity.[32] Figure S2 shows the change in adsorption capacity of MB because of the presence of competing ions. Obviously, the addition of NaCl causes a reduction in the removal rate of MB, and a further increase in the amount of NaCl has a significant effect on the results. This is because the Na^+ and Cl^- ions in the solution can affect the electrostatic interaction between the adsorbent and the target contaminant.[33] Therefore, the decrease in adsorption capacity is due to the fact that a large amount of positively charged Na ions in the solution compete with MB at the same time for the active sites on the adsorbent.

Adsorption Kinetic Study. The adsorption mechanism is provided by adsorption kinetics which is of a great significance in wastewater treatment.[34] To evaluate the mechanism of MB dye adsorption onto TA−PVA/SA hydrogel beads, the pseudo-first-order and pseudo-second-order kinetics were employed to interpret the experimental data, as shown in eqs 1 and 2.

Pseudo-first-order model[35]

$$\log(q_e - q_t) = \log\ q_e - k_1 t/2.303 \quad (1)$$

Pseudo-second-order model[36]

$$t/q_t = 1/(k_2 q_e^{\ 2}) + t/q_e \quad (2)$$

where k_1 (h^{-1}) and k_2 (g/mg h) are the rate constants of pseudo-first-order and pseudo-second-order adsorption, respectively.

Figure 5a shows the relationship between time and $\log(q_e - q_t)$ or t/q_t. The rate constants and the corresponding R^2 values of pseudo-first-order and pseudo-second-order are given in the Table 1. The pseudo-second-order model provides better correlation coefficients than that of pseudo-first-order model, and the q_e values are in good agreement with experimental q_e values which suggests that the MB dye followed the pseudo-second-order kinetic model.

Intraparticle Diffusion Study. The adsorption process can be divided into different steps, including the transfer of the target contaminants to the surface of the adsorbent particles, then to the active center of the adsorbent, and finally immobilize on the active site through adsorption and complexation.[37] Intraparticle diffusion can reflect changes in the removal rate of a target contaminant. Therefore, the Weber−Morris equation eq 3 could be used to identify the controlled rate, as follows[38]

$$q_t = k_{id} t^{1/2} + C \quad (3)$$

where k_{id} (mg/g $min^{0.5}$) is the intraparticle diffusion rate constant and C is the intercept.

Figure 5b shows the linear-fitted intraparticle diffusion model image, and the data obtained in the process of MB removal is presented in Table 2, implying that three steps had

Table 2. Parameters of Intraparticle Diffusion Model for MB Removal by TA−PVA/SA Hydrogel Beads

	K_{id} (mg/g $min^{1/2}$)	C	R^2
part I	11.09	2.91	0.9728
part II	2.91	75.51	0.9496
part III	0.15	136.96	0.7798

happened. On the first stage, it is a rapid process on adsorption, which can be attributed to the fact that many active sites in the TA−PVA/SA hydrogel beads can be occupied by MB molecules. As the adsorption amount increases, the active sites on the TA−PVA/SA hydrogel beads decrease; the adsorption is going to the second portion, whose rate is limited by diffusion.[39] In the last part, the adsorption capacities is almost constant because the adsorbent sites are almost entirely occupied at equilibrium.

Adsorption Isotherm Study. The isotherm models of Langmuir and Freundlich are employed to get more insights into the removal process of MB dye by TA−PVA/SA hydrogel beads. The Langmuir isotherm model is assumed to have affinity for monolayer adsorption. The adsorbent surface has the same active site and the adsorption energy.[40] Whereas the Freundlich isotherm model is used to understand the adsorption of multiple adsorption layer surfaces.[41] They can be expressed as the following equations, respectively.

Langmuir isotherms[42]

$$C_e/q_e = 1/(K_L q_m) + C_e/q_e \quad (4)$$

Freundlich isotherms[43]

$$\log\ q_e = \log\ K_F + 1/n \log C_e \quad (5)$$

where q_m (mg/g) is the maximum amount of MB adsorbed per unit weight of the adsorbent and K_L (L/mg) is the constant related to the maximum removal energy. K_F (mg/g)/(mg/L)$^{1/n}$ and n are the Freundlich constants related to the adsorption capacity and adsorption intensity, respectively. Figure 5c displays the adsorption isotherms of the MB removal from solution by the TA−PVA/SA hydrogel beads. In addition, the corresponding parameters of the models and the fitted equilibrium data are presented in Table 3. Results showed that the Langmuir model gave a better description of adsorption than the Freundlich model with $R^2 > 0.99$ and the

DOI: 10.1021/acsomega.8b00577
ACS Omega 2018, 3, 7523−7531

Table 3. Parameters of Isotherm Models for MB Removal from Solution by TA−PVA/SA Hydrogel Beads

	Langmuir isotherm model			Freundlich isotherm model		
adsorbate	K_L (L/mg)	q_m (mg/g)	R^2	K_F (mg/g)/(mg/L)$^{1/n}$	$1/n$	R^2
MB	0.26	147.06	0.9960	36.64	0.33	0.85

q_m reaching 147.06 mg/g. The Freundlich model, whose R^2 values (0.85) are not close enough to 1, was demonstrated such that it is unable to predict the adsorption data process.

Thermodynamic Study. To understand the thermodynamic properties of the MB dye adsorption process, thermodynamic parameters such as standard entropy ($\Delta S°$), standard enthalpy ($\Delta H°$), and standard Gibbs free energy ($\Delta G°$) were calculated. Their relations are expressed by the equations as[44]

$$K_c = q_e/C_e \quad (6)$$

$$\Delta G° = -RT \ln K_c \quad (7)$$

$$\ln K_c = \Delta S°/R - \Delta H°/RT \quad (8)$$

where, K_c is the equilibrium constant and R (8.314 J/mol K) is the gas constant. q_e (mg/g) and C_e (mg/L) are the adsorption amount and equilibrium concentration, respectively. The $\Delta H°$ and $\Delta S°$ were gained from the slope and intercept of plot between ln K_c and $1/T$[45] and these parameters are listed in Table 4. The values of $\Delta G°$ are all less than zero for all studied temperature ranges, indicating the spontaneous and viable nature of the adsorption properties. $\Delta H°$ is a negative value, indicating that adsorption of MB dye by TA−PVA/SA hydrogel beads is exothermic.

Table 4. Thermodynamic Parameters of MB Adsorption on TA−PVA/SA Hydrogel Beads

temperature (K)	$\Delta G°$ (kJ/mol)	$\Delta H°$ (kJ/mol)	$\Delta S°$ (J/mol K)
		−24.13	−72.23
293	−2.89		
303	−2.20		
313	−1.57		

Reusability of Adsorbent. The TA−PVA/SA hydrogel beads for the dyes are reused for 5 cycles which are washed by 0.1 mol/L HCl solution as the eluent. In Figure 6, the first adsorption capacity is 123.06 mg/g, which is better than that of other cycles. However, with the increase in the number of cycles, the adsorption amount can be maintained at a steady value about 100 mg/g. It is clearly observed that the TA−PVA/SA hydrogel beads had effective properties for MB absorption compared with other adsorbents of others (Table 5).

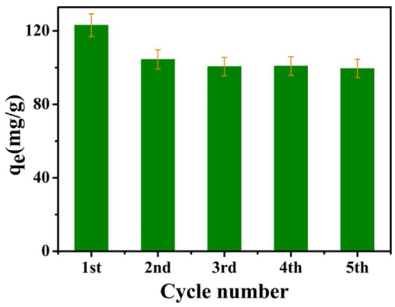

Figure 6. Recyclability of TA−PVA/SA hydrogel beads adsorbent for dye removal (C_0[MB] = 120 mg/L, V = 100 mL, t = 12 h, pH = 9, dos. = 50 mg, and T = 30 °C).

Table 5. Comparison of the Maximum Capacities with the Previous Adsorbents in Literature

	adsorbate		
adsorbent	MB (mg/g)	pH	references
modified ball clay	100.0	11	46
PVA	123.30	6	17
iron−TA complexes	67.41	9	47
halloysite nanotubes	40.82	10	48
TA-modified Fe_3O_4 nanoparticles	90.90	10	49
cellulose nanocrystals	118	10	50
TA−PVA/SA	147.06	9	this work

CONCLUSIONS

The TA−PVA/SA hydrogel beads are easily prepared, and the removal ability is probed by MB dye from simulated sewage. The experimental results show that TA content plays an important role in the adsorption of MB by TA−PVA/SA hydrogel beads whose maximum removal amount reaches 147.06 mg/g which is much better than that without TA. The adsorption processes are well-described by the pseudo-second-order model and the experimental data fit the Langmuir isotherm well. According to thermodynamic studies analysis, TA−PVA/SA hydrogel beads removal of MB from simulated sewage is a spontaneous process with exothermic properties. After five cycles of analysis, TA−PVA/SA hydrogel beads still maintain good performance in removing MB dye. Therefore, the new hydrogel beads are provided to remove dyes such as MB from wastewater.

EXPERIMENTAL SECTION

Materials. All chemicals are used without further purification. TA (water soluble) was purchased from Aladdin. SA (AR), PVA (M_n = 80 000, AR), $CaCl_2$, and boric acid were purchased from Chemical Reagent Factory of Tianjin, China. MB, a cationic dye with a molecular formula ($C_{16}H_{18}ClN_3S·3H_2O$), as shown in Figure 7, was supplied by Aladdin and used as adsorbate. The ultrapure water (UW) (18.25 MΩ·cm) was used in all experiments.

Preparation of TA−PVA/SA Hydrogel Beads. The TA−PVA/SA hydrogel bead adsorbents were prepared by the following steps: PVA (2.0 g) and SA (0.26 g) were placed into a flask filled with 50 mL of UW under mechanical stirring in a 95 °C water bath for 1 h. After complete dissolving, the solution was stirred for an addition of 3 h at 65 °C. The TA solution was prepared by adding 0.22 g of TA to 10 mL of UW under ultrasonic dispersion for 15 min at 25 °C and then added dropwise to the above mixture, and continued to stir for 1 h at 65 °C. The appellant mixed solution was slowly added dropwise to the stirring of 3% $CaCl_2$-saturated boric acid solution by a syringe (Figure 8). The TA−PVA/SA hydrogel

DOI: 10.1021/acsomega.8b00577
ACS Omega 2018, 3, 7523−7531

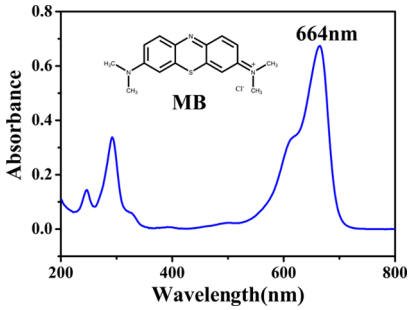

Figure 7. Molecular formula and UV−visible spectrum of MB.

beads were thoroughly washed by UW and dried in a vacuum freeze-drying machine.

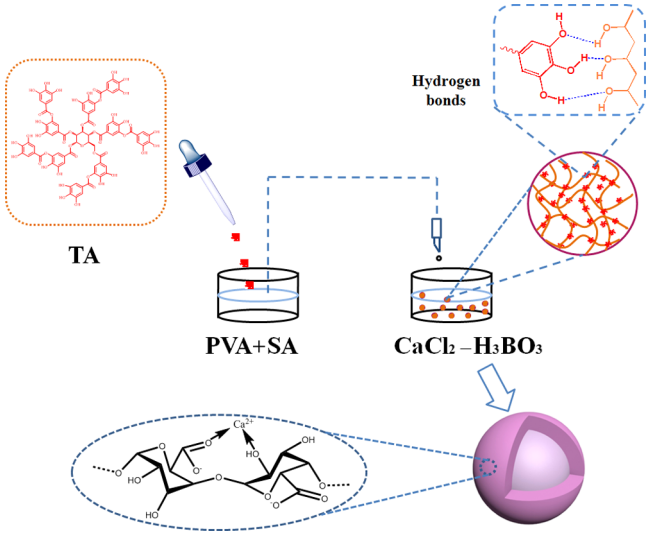

Figure 8. Preparation process and possible mechanism of TA−PVA/SA hydrogel bead adsorbents.

Characterization. The structure of the samples and the chemical composition were characterized by the FT-IR (Nicolet iS10, America). Determination of thermal stability of samples by TGA (Mettler-Toledo, Switzerland) from 45 to 800 °C under nitrogen flow (20 mL/min) with 10 °C/min. The microscopic appearance of the samples was observed by SEM (FSM-5600LV, Japan) at 20 kV. The chemical composition of the samples was subjected to XPS (Thermo Scientific, USA) analysis using Al Kα radiation. The concentration of solutions before and after adsorption was measured with an ultraviolet spectrophotometer (UV-2550, Shimadzu, Japan).

MB Adsorption and Desorption. The adsorption of MB from aqueous solution onto TA−PVA/SA beads composite was systematically evaluated. Before adsorption experiment, a series of diluted MB solutions were prepared with UW and were analyzed by a UV spectrophotometer which records characteristic absorption peak of MB at 664 nm. First, a certain amount of adsorbent was added to a 150 mL Erlenmeyer flask having a certain concentration (100 mL) and placed in an isothermal water bath shaker at 190 rpm. After a period of time, the supernatant was centrifuged and the concentration was measured with an ultraviolet spectrophotometer. Effect of different TA content (0−0.22 g), different pH (2−10), TA−PVA/SA dosage (50−125 mg), contact time (0−48 h), initial MB concentration (0−160 mg/L), and temperature (20, 30, and 40 °C) have been explored to evaluate the performance of sorbents. Then, the adsorption capacity was calculated using eq 9[51]

$$q_t = (C_0 - C_t)V/m \quad (9)$$

where q_t (mg/g) is the adsorbed amount after time t, C_0 and C_t (mg/L) are the initial concentration and remaining concentration after time t, respectively. V (mL) is the volume of MB solution and m (mg) is the weight of TA−PVA/SA beads.

The reusability of TA−PVA/SA adsorbent was carried out in the repeating adsorption−desorption process. TA−PVA/SA beads (0.05 g) after adsorbing MB were placed in a glass bottle containing 0.1 mol/L HCl solution (100 mL). After shaking for 1 h, the TA−PVA/SA beads were separated from the solution and used for the following adsorption.

■ ASSOCIATED CONTENT

Supporting Information

The Supporting Information is available free of charge on the ACS Publications website at DOI: 10.1021/acsomega.8b00577.

Chromogenic reaction of TA−PVA/SA with $FeCl_3$: TA−PVA/SA hydrogel beads soaked in pure water, color reaction of dropping $FeCl_3$ and effect of competitive ions on MB removal (C_0[MB] = 120 mg/L, V = 100 mL, t = 12 h, pH = 9, dos. = 50 mg, T = 30 °C) (PDF)

■ AUTHOR INFORMATION

Corresponding Authors

*E-mail: liuqinze@qlu.edu.cn (Q.L.).
*E-mail: yaojsh@qlu.edu.cn (J.Y.).

ORCID

Qinze Liu: 0000-0002-2240-9320

Notes

The authors declare no competing financial interest.

■ ACKNOWLEDGMENTS

The authors greatly acknowledge the support of the Opening program of State Key Laboratory of Solid Lubrication (LSL-1508), the National Natural Science Foundation of China (grant no. 51303086, 51503108, 51503107, 51605470), and the Foundation (no. KF201602) of Key Laboratory of Pulp and Paper Science and Technology of Ministry of Education/Shandong Province of China.

■ REFERENCES

(1) Asfaram, A.; Ghaedi, M.; Goudarzi, A.; Rajabi, M. Response surface methodology approach for optimization of simultaneous dye and metal ion ultrasound-assisted adsorption onto Mn doped Fe3O4-NPs loaded on AC: kinetic and isothermal studies. *Dalton Trans.* **2015**, *44*, 14707−14723.

(2) Kadirvelu, K.; Kavipriya, M.; Karthika, C.; Radhika, M.; Vennilamani, N.; Pattabhi, S. Utilization of various agricultural wastes for activated carbon preparation and application for the removal of dyes and metal ions from aqueous solutions. *Bioresour. Technol.* **2003**, *87*, 129−132.

(3) Singh, K. P.; Gupta, S.; Singh, A. K.; Sinha, S. Optimizing adsorption of crystal violet dye from water by magnetic nanocomposite using response surface modeling approach. *J. Hazard. Mater.* **2011**, *186*, 1462−1473.

DOI: 10.1021/acsomega.8b00577
ACS Omega 2018, 3, 7523−7531

(4) Roosta, M.; Ghaedi, M.; Daneshfar, A.; Sahraei, R.; Asghari, A. Optimization of the ultrasonic assisted removal of methylene blue by gold nanoparticles loaded on activated carbon using experimental design methodology. *Ultrason. Sonochem.* **2014**, *21*, 242−252.
(5) Liang, C.-Z.; Sun, S.-P.; Li, F.-Y.; Ong, Y.-K.; Chung, T.-S. Treatment of highly concentrated wastewater containing multiple synthetic dyes by a combined process of coagulation/flocculation and nanofiltration. *J. Membr. Sci.* **2014**, *469*, 306−315.
(6) Türgay, O.; Ersöz, G.; Atalay, S.; Forss, J.; Welander, U. The treatment of azo dyes found in textile industry wastewater by anaerobic biological method and chemical oxidation. *Sep. Purif. Technol.* **2011**, *79*, 26−33.
(7) Liang, H.-W.; Cao, X.; Zhang, W.-J.; Lin, H.-T.; Zhou, F.; Chen, L.-F.; Yu, S.-H. Robust and highly efficient free-standing carbonaceous nanofiber membranes for water purification. *Adv. Funct. Mater.* **2011**, *21*, 3851−3858.
(8) Pan, C.; Zhu, Y. New Type of BiPO4Oxy-Acid Salt Photocatalyst with High Photocatalytic Activity on Degradation of Dye. *Environ. Sci. Technol.* **2010**, *44*, 5570−5574.
(9) Chaudhuri, H.; Dash, S.; Sarkar, A. Single-step room-temperature in situ syntheses of sulfonic acid functionalized SBA-16 with ordered large pores: potential applications in dye adsorption and heterogeneous catalysis. *Ind. Eng. Chem. Res.* **2017**, *56*, 2943−2957.
(10) Zhao, X.; Wang, K.; Gao, Z.; Gao, H.; Xie, Z.; Du, X.; Huang, H. Reversing the Dye Adsorption and Separation Performance of Metal-Organic Frameworks via Introduction of −SO3H Groups. *Ind. Eng. Chem. Res.* **2017**, *56*, 4496−4501.
(11) Tanhaei, B.; Ayati, A.; Lahtinen, M.; Sillanpää, M. Preparation and characterization of a novel chitosan/Al2O3/magnetite nanoparticles composite adsorbent for kinetic, thermodynamic and isotherm studies of Methyl Orange adsorption. *Chem. Eng. J.* **2015**, *259*, 1−10.
(12) Li, J.; Xu, Z.; Wu, W.; Jing, Y.; Dai, H.; Fang, G. Nanocellulose/Poly(2-(dimethylamino)ethyl methacrylate)Interpenetrating polymer network hydrogels for removal of Pb(II) and Cu(II) ions. *Colloids Surf., A* **2018**, *538*, 474−480.
(13) Zhou, C.; Wu, Q.; Lei, T.; Negulescu, I. I. Adsorption kinetic and equilibrium studies for methylene blue dye by partially hydrolyzed polyacrylamide/cellulose nanocrystal nanocomposite hydrogels. *Chem. Eng. J.* **2014**, *251*, 17−24.
(14) Peng, Q.; Liu, M.; Zheng, J.; Zhou, C. Adsorption of dyes in aqueous solutions by chitosan-halloysite nanotubes composite hydrogel beads. *Microporous Mesoporous Mater.* **2015**, *201*, 190−201.
(15) Li, C.; She, M.; She, X.; Dai, J.; Kong, L. Functionalization of polyvinyl alcohol hydrogels with graphene oxide for potential dye removal. *J. Appl. Polym. Sci.* **2014**, *131*, 39872.
(16) Gupta, V. K.; Tyagi, I.; Agarwal, S.; Sadegh, H.; Shahryari-ghoshekandi, R.; Yari, M.; Yousefi-nejat, O. Experimental study of surfaces of hydrogel polymers HEMA, HEMA-EEMA-MA, and PVA as adsorbent for removal of azo dyes from liquid phase. *J. Mol. Liq.* **2015**, *206*, 129−136.
(17) Agarwal, S.; Sadegh, H.; Monajjemi, M.; Hamdy, A. S.; Ali, G. A. M.; Memar, A. O. H.; Shahryari-ghoshekandi, R.; Tyagi, I.; Gupta, V. K. Efficient removal of toxic bromothymol blue and methylene blue from wastewater by polyvinyl alcohol. *J. Mol. Liq.* **2016**, *218*, 191−197.
(18) Tong, S.; Zhao, S.; Zhou, W.; Li, R.; Jia, Q. Modification of multi-walled carbon nanotubes with tannic acid for the adsorption of La, Tb and Lu ions. *Microchim. Acta* **2011**, *174*, 257−264.
(19) Fu, J.; Chen, Z.; Wang, M.; Liu, S.; Zhang, J.; Zhang, J.; Han, R.; Xu, Q. Adsorption of methylene blue by a high-efficiency adsorbent (polydopamine microspheres): Kinetics, isotherm, thermodynamics and mechanism analysis. *Chem. Eng. J.* **2015**, *259*, 53−61.
(20) Liao, X.; Lu, Z.; Zhang, M.; Liu, X.; Shi, B. Adsorption of Cu(II) from aqueous solutions by tannins immobilized on collagen. *J. Chem. Technol. Biotechnol.* **2004**, *79*, 335−342.
(21) Bertagnolli, C.; Grishin, A.; Vincent, T.; Guibal, E. Boron removal by a composite sorbent: Polyethylenimine/tannic acid derivative immobilized in alginate hydrogel beads. *J. Environ. Sci. Health, Part A: Toxic/Hazard. Subst. Environ. Eng.* **2016**, *52*, 359−367.
(22) Xu, R.; Ma, S.; Lin, P.; Yu, B.; Zhou, F.; Liu, W. High Strength Astringent Hydrogels Using Protein as the Building Block for Physically Cross-linked Multi-Network. *ACS Appl. Mater. Interfaces* **2018**, *10*, 7593−7601.
(23) Xia, Z.; Singh, A.; Kiratitanavit, W.; Mosurkal, R.; Kumar, J.; Nagarajan, R. Unraveling the mechanism of thermal and thermo-oxidative degradation of tannic acid. *Thermochim. Acta* **2015**, *605*, 77−85.
(24) Becerril, H. A.; Mao, J.; Liu, Z.; Stoltenberg, R. M.; Bao, Z.; Chen, Y. Evaluation of solution-processed reduced graphene oxide films as transparent conductors. *ACS Nano* **2008**, *2*, 463−470.
(25) Crini, G.; Peindy, H.; Gimbert, F.; Robert, C. Removal of C.I. Basic Green 4 (Malachite Green) from aqueous solutions by adsorption using cyclodextrin-based adsorbent: Kinetic and equilibrium studies. *Sep. Purif. Technol.* **2007**, *53*, 97−110.
(26) Malash, G. F.; El-Khaiary, M. I. Methylene blue adsorption by the waste of Abu-Tartour phosphate rock. *J. Colloid Interface Sci.* **2010**, *348*, 537−545.
(27) Huang, Z.-H.; Zheng, X.; Lv, W.; Wang, M.; Yang, Q.-H.; Kang, F. Adsorption of lead(II) ions from aqueous solution on low-temperature exfoliated graphene nanosheets. *Langmuir* **2011**, *27*, 7558−7562.
(28) Kampalanonwat, P.; Supaphol, P. Preparation and adsorption behavior of aminated electrospun polyacrylonitrile nanofiber mats for heavy metal ion removal. *ACS Appl. Mater. Interfaces* **2010**, *2*, 3619−3627.
(29) Ullah, I.; Nadeem, R.; Iqbal, M.; Manzoor, Q. Biosorption of chromium onto native and immobilized sugarcane bagasse waste biomass. *Ecol. Eng.* **2013**, *60*, 99−107.
(30) Liu, Q.; Liu, Q.; Wu, Z.; Wu, Y.; Gao, T.; Yao, J. Efficient removal of methyl orange and alizarin red S from pH-unregulated aqueous solution by the catechol-amine resin composite using hydrocellulose as precursor. *ACS Sustainable Chem. Eng.* **2017**, *5*, 1871−1880.
(31) Ho, Y.-S.; Chiu, W.-T.; Wang, C.-C. Regression analysis for the sorption isotherms of basic dyes on sugarcane dust. *Bioresour. Technol.* **2005**, *96*, 1285−1291.
(32) Zhang, Q.; Li, Y.; Yang, Q.; Chen, H.; Chen, X.; Jiao, T.; Peng, Q. Distinguished Cr(VI) capture with rapid and superior capability using polydopamine microsphere: Behavior and mechanism. *J. Hazard. Mater.* **2018**, *342*, 732−740.
(33) Doğan, M.; Abak, H.; Alkan, M. Biosorption of Methylene Blue from Aqueous Solutions by Hazelnut Shells: Equilibrium, Parameters and Isotherms. *Water, Air, Soil Pollut.* **2008**, *192*, 141−153.
(34) Niu, Y.; Qu, R.; Sun, C.; Wang, C.; Chen, H.; Ji, C.; Zhang, Y.; Shao, X.; Bu, F. Adsorption of Pb(II) from aqueous solution by silica-gel supported hyperbranched polyamidoamine dendrimers. *J. Hazard. Mater.* **2013**, *244−245*, 276−286.
(35) Ho, Y.; McKay, G. The kinetics of sorption of divalent metal ions onto sphagnum moss peat. *Water Res.* **2000**, *34*, 735−742.
(36) Zhao, J.; Ge, S.; Liu, L.; Shao, Q.; Mai, X.; Zhao, C. X.; Hao, L.; Wu, T.; Yu, Z.; Guo, Z. Microwave solvothermal fabrication of zirconia hollow microspheres with different morphologies using pollen templates and their dye adsorption removal. *Ind. Eng. Chem. Res.* **2017**, *57*, 231−241.
(37) Shroff, K. A.; Vaidya, V. K. Kinetics and equilibrium studies on biosorption of nickel from aqueous solution by dead fungal biomass of Mucor hiemalis. *Chem. Eng. J.* **2011**, *171*, 1234−1245.
(38) Dash, S.; Chaudhuri, H.; Gupta, R.; Nair, U. G.; Sarkar, A. Fabrication and application of low-cost thiol functionalized coal fly ash for selective adsorption of heavy toxic metal ions from water. *Ind. Eng. Chem. Res.* **2017**, *56*, 1461−1470.
(39) Duran, C.; Ozdes, D.; Gundogdu, A.; Senturk, H. B. Kinetics and isotherm analysis of basic dyes adsorption onto almond shell (prunus dulcis) as a low cost adsorbent. *J. Chem. Eng. Data* **2011**, *56*, 2136−2147.

DOI: 10.1021/acsomega.8b00577
ACS Omega 2018, 3, 7523−7531

(40) Elabbas, S.; Mandi, L.; Berrekhis, F.; Pons, M. N.; Leclerc, J. P.; Ouazzani, N. Removal of Cr(III) from chrome tanning wastewater by adsorption using two natural carbonaceous materials: Eggshell and powdered marble. *J. Environ. Manage.* **2016**, *166*, 589−595.
(41) Puddu, V.; Perry, C. C. Peptide adsorption on silica nanoparticles: evidence of hydrophobic interactions. *ACS Nano* **2012**, *6*, 6356−6363.
(42) Yu, R.; Shi, Y.; Yang, D.; Liu, Y.; Qu, J.; Yu, Z.-Z. Graphene oxide/chitosan aerogel microspheres with honeycomb-cobweb and radially oriented microchannel structures for broad-spectrum and rapid adsorption of water contaminants. *ACS Appl. Mater. Interfaces* **2017**, *9*, 21809−21819.
(43) Dehghani, M. H.; Taher, M. M.; Bajpai, A. K.; Heibati, B.; Tyagi, I.; Asif, M.; Agarwal, S.; Gupta, V. K. Removal of noxious Cr (VI) ions using single-walled carbon nanotubes and multi-walled carbon nanotubes. *Chem. Eng. J.* **2015**, *279*, 344−352.
(44) Lei, C.; Zhu, X.; Zhu, B.; Jiang, C.; Le, Y.; Yu, J. Superb adsorption capacity of hierarchical calcined Ni/Mg/Al layered double hydroxides for Congo red and Cr(VI) ions. *J. Hazard. Mater.* **2017**, *321*, 801−811.
(45) Gholipour, M.; Hashemipour, H.; Mollashahi, M. Hexavalent chromium removal from aqueous solution via adsorption on granular activated carbon: Adsorption, desorption, modeling and simulation studies. *J. Eng. Appl. Sci.* **2011**, *6*, 10−18.
(46) Auta, M.; Hameed, B. H. Modified mesoporous clay adsorbent for adsorption isotherm and kinetics of methylene blue. *Chem. Eng. J.* **2012**, *198−199*, 219−227.
(47) Li, Y. M.; Miao, X.; Wei, Z. G.; Cui, J.; Li, S. Y.; Han, R. M.; Zhang, Y.; Wei, W. Iron-tannic acid nanocomplexes: facile synthesis and application for removal of methylene blue from aqueous solution. *Dig. J. Nanomater. Bios* **2016**, *11*, 1045−1061.
(48) Zhao, M.; Liu, P. Adsorption behavior of methylene blue on halloysite nanotubes. *Microporous Mesoporous Mater.* **2008**, *112*, 419−424.
(49) Abkenar, S. D.; Khoobi, M.; Tarasi, R.; Hosseini, M.; Shafiee, A.; Ganjali, M. R. Fast Removal of Methylene Blue from Aqueous Solution Using Magnetic-Modified Fe3O4 Nanoparticles. *J. Environ. Eng.* **2015**, *141*, 04014049.
(50) Batmaz, R.; Mohammed, N.; Zaman, M.; Minhas, G.; Berry, R. M.; Tam, K. C. Cellulose nanocrystals as promising adsorbents for the removal of cationic dyes. *Cellulose* **2014**, *21*, 1655−1665.
(51) Zhu, K.; Gao, Y.; Tan, X.; Chen, C. Polyaniline-modified Mg/Al layered double hydroxide composites and their application in efficient removal of Cr(VI). *ACS Sustainable Chem. Eng.* **2016**, *4*, 4361−4369.

DOI: 10.1021/acsomega.8b00577
ACS Omega 2018, 3, 7523−7531